A closure for the Ornstein-Zernike equation with pressure and free energy consistency

Tsogbayar Tsednee
Department of Physics and Astronomy, California State University Northridge, 18111 Nordhoff Street, Northridge, CA 91333, USA

Tyler Luchko*
(Dated: September 15, 2022)

The Ornstein-Zernike (OZ) integral equation theory is a powerful approach to simple liquids due to its low computational cost and the fact that, when combined with an appropriate closure equation, the theory is thermodynamically complete. However, approximate closures proposed to date exhibit pressure or free energy inconsistencies that produce inaccurate or ambiguous results, limiting the usefulness of the Ornstein-Zernike approach. To address this problem, we have developed a new closure approximation that simultaneously enforces both pressure and free energy consistency and tests it for a single-component Lennard-Jones fluid. The closure is a simple power series in the direct and total correlation functions for which we have derived analytical formulas for the excess Helmholtz free energy and chemical potential. These expressions contain a partial molar volume-like term, similar to excess chemical potential correction terms recently developed. Using our new bridge approximation, we have calculated the pressure, Helmholtz free energy, and chemical potential for the Lennard-Jones fluid using the Kirkwood charging, thermodynamic integration techniques, and analytic expressions. These results are compared with those from the hypernetted chain equation and the Verlet-modified closure against Monte Carlo and equations-of-state data for reduced densities of $\rho^* < 1$ and temperatures of $T^* = 1.5$, 2.74, and 5. Our new closure shows consistency among all thermodynamic paths, except for one expression of the Gibbs-Duhem relation, whereas the hypernetted chain equation and Verlet-modified closure only exhibit consistency between a few relations. Accuracy of the new closure is comparable to Verlet-modified closure and a significant improvement to results obtained from the hypernetted chain equation.

I. INTRODUCTION

Integral equation and classical density functional theories of the statistical mechanics of liquids have increasingly been used in the study of biological and condensed matter systems due to their low computational cost and the physical insights they provide. Over the years, fundamental theories, such as the Ornstein-Zernike (OZ) equation [1] and classical density functional theory (CDFT) [2], have been developed to deal with complex solutes and molecular solvents; e.g., reference interaction site model (RISM) theories [3–7], molecular OZ[8, 9], and molecular CDFT [10]. Common to all these theories is the requirement of a closure relation. Unfortunately, approximations to the closure equation invariably introduce path-dependencies to state variables – i.e., thermodynamic inconsistencies – that should not exist. Importantly, quantitatively different pressures and free energies are calculated when different thermodynamic routes are employed. Such inconsistencies limit the physical insights that can be gained and affect the accuracy of the theory. This has not gone unnoticed by the community and a variety of methods have been developed to remove different path dependencies. Despite an immense amount of work on the subject, no closure approximation has been developed that incorporates both free energy and pressure consistency.

A popular approach to addressing pressure inconsistencies found in early closures has been to enforce pressure consistency. In this approach, the approximate closure contains one or more free parameters, which are adjusted to ensure density derivatives of the pressure calculated from the virial and compressibility paths agree. Examples of this approach includes closures due to Verlet [11, 12], Martynov-Sarkisov (MS) [13], Rogers-Young (RY) [14], Zerah-Hansen (ZH) [15], and Balloni-Pastore-Galli-Gazillo (BPGG) [16], Martynov and Vompe (MV) [17], Duh and Haymet (DH) [18], and Lee [19]. While these closures have had success in improving the prediction of pressure and some other state variables, free energies and chemical potentials have been approximated and path-independence has not been conclusively shown. In fact, for several closures path-dependence has been clearly demonstrated [20–23].

Insights to the problem of free energy inconsistencies were provided by Kast [24], who derived sufficient conditions for a closure to be path independent. While satisfying Kast's conditions is not required for path-independence, only the partial series expansion of order-n (PSE-n) [25] closures, which includes HNC [26] and Kovalenko-Hirata (KH) [7] closures, have been shown to satisfy them. Indeed, nearly all other closures in the literature explicitly depend on the indirect correlation function or modifications to the potential energy function and exhibit path dependence. However, PSE-n closures do not display pressure consistency and provide inaccurate pressure estimates [27], which affects the accuracy of the free energy prediction. In fact,

* tluchko@csun.edu

to compensate for the large pressure errors, a number of partial molar volume (PMV) corrections have been developed for use with 3D-RISM and mDFT theories [28–31].

In this work, we combine both approaches by proposing a closure approximation that both satisfies the Kast path-independence criteria for the free Helmholtz energy and has adjustable parameters through which pressure consistency may be enforced. We show that this closure not only satisfies both pressure and free energy consistency relations but also internal energy-pressure, free-energy pressure, and Gibbs-Duhem consistency. Furthermore, we derived analytic, closed-form formulas for both the chemical potential and Helmholtz free energy for a simple Lennard-Jones (LJ) fluid. This formula for the chemical potential is functionally similar to the HNC relation with the Universal Correction [28] applied. To demonstrate the effectiveness of this approach, we present results for pressure for the LJ potential at densities $\rho\sigma^3 = 0.1$ to 1.1, and temperatures $T^* = 1.5, 2.74$ and 5 in reduced units using the HNC, the Verlet-modified (VM) [32], and our new bridge function approximation. Several consistency relations are checked for all three approximations and results for the excess free energy and excess chemical potential are compared with available simulation and equation of state data [33–35].

The paper is organized as follows. In Section II we discuss theoretical formulations for obtaining the correlation functions for the LJ fluid, the bridge functions, thermodynamic consistency and path dependence. In this section we also discuss calculations of the excess chemical potential and excess Helmholtz free energy. Numerical procedures used to calculate thermodynamic quantities are described in Section III. In Section IV we present our results and in Section V we discuss them, followed by conclusions.

II. THEORY

Ornstein-Zernike equation

Many excellent descriptions of the OZ equation can be found in the literature such as [36, 37]. Briefly, the OZ equation divides the contributions to equilibrium liquid structure into direct and indirect contributions. For a homogeneous and a single component system at temperature T and number density ρ, it may be written in the form

$$h(r) = c(r) + \rho \int c(|\boldsymbol{r} - \boldsymbol{r'})h(\boldsymbol{r'})d\boldsymbol{r'} \tag{1}$$

where $h(r)$ and $c(r)$ are the total and the direct correlation functions, respectively. With these functions, one can define the indirect correlation, $\gamma \equiv h(r) - c(r)$, and radial distribution functions, $g(r) = h(1) + 1$.

To solve Eq. (1), one needs a second equation called a *closure relation*, that relates the correlation functions to a spherically symmetric pair potential $u(r)$ between the liquid particles. This closure equation is defined as

$$h(r) = \exp[-\beta u(r) + \gamma(r) + B(r)] - 1, \tag{2}$$

where $B(r)$ is the bridge function, $\beta = 1/k_{\mathrm{B}}T$, and k_{B} is the Boltzmann constant. $B(r)$ can be expressed as a power series in ρ of irreducible diagrams [38] but, in practice, is approximated as some combination of $u\,(r)$, $h\,(r)$, and $c\,(r)$. By solving Eqs. (1) and (2) self-consistently, both correlation functions may be obtained. Commonly used closures include the HNC,

$$B_{\mathrm{HNC}}(r) = 0, \tag{3}$$

and a VM approximation [32],

$$B_{\mathrm{VM}}(r) = -\frac{1}{2}\frac{\phi\gamma_a^2}{1 + \alpha\gamma_a}, \tag{4}$$

where ϕ and α are free parameters to be optimized. Here $\gamma_a \equiv \gamma - \beta u_a$ and $u_a(r)$ is the attractive part of the pair potential discussed by Weeks, Chandler and Andersen [39].

Thermodynamic quantities

Once the pair distribution function $g(r)$ is obtained, thermodynamic quantities of interest can be computed. The pressure from the virial equation of state, p^v, [36] is computed as,

$$\frac{\beta p^v}{\rho} = 1 - \frac{\rho}{6}\int d\boldsymbol{r} r \frac{\partial \beta u(r)}{\partial r} g(r), \tag{5}$$

where $\beta = 1/k_bT$, k_b is Boltzmann's constant and T is temperature. The isothermal compressibility, χ_T, is computed through the compressibility route [36],

$$\beta(\rho\chi_T)^{-1} = \beta\left(\frac{\partial p^c}{\partial \rho}\right)_T = 1 - \rho\int c(r)d\boldsymbol{r} \tag{6}$$

where p^c is the pressure from the compressibility route and the pressure can be computed as

$$\frac{\beta p^c}{\rho} = \frac{\beta}{\rho}\int_0^\rho d\rho' \rho'^{-1}\chi_T^{-1}. \tag{7}$$

The internal energy may be directly computed as

$$\begin{aligned} E &= E^i + E^e \\ &= \frac{3}{2}k_bT + \frac{\rho}{2}\int g\,(\mathbf{r})\,u\,(\mathbf{r})\,\mathrm{d}\mathbf{r} \end{aligned} \tag{8}$$

where E^e is the excess internal energy and E^i is the internal energy of the ideal gas.

Calculation of the excess Helmholtz free energy

The most common technique of handling the free energy is the Kirwood charging technique [40, 41], in which the free energy difference between two different states represented with two different Hamiltonians is calculated by gradually "switching between" the Hamiltonians using the coupling parameter λ . When $\lambda = 0$, the system is represented by a Hamiltonian corresponding to the initial state, and for $\lambda = 1$ by a Hamiltonian corresponding to the final state. By gradually turning on interactions between all N particle at once, the system may stay at a given temperature T. Then the excess Helmholtz free energy, A^e, is obtained in terms of thermodynamic integration with the Kirkwood charging formula,

$$\frac{\beta A^e}{N} = \frac{\rho}{2}\int_0^1 d\lambda \int d\boldsymbol{r} \frac{\partial \beta u(r,\lambda)}{\partial \lambda} g(r,\lambda). \tag{9}$$

Another approach to calculating the free energy, which also represents another thermodynamic path, is to integrate from zero to the desired density [34, 42]

$$\frac{\beta A^e}{N} = \int_0^\rho \frac{1}{\rho'}\Big(\frac{\beta p}{\rho'} - 1\Big) d\rho'. \tag{10}$$

When this is evaluated numerically, the pressure must be calculated at each intermediate density.

Calculation of the excess chemical potential

As with the Helmholtz free energy, there are numerous physical and non-physical paths to the excess chemical potential, μ^e, (i.e., the Gibbs free energy per particle). Again, the commonly used Kirkwood charging formula [40, 41] may be applied,

$$\beta\mu^e = \rho\int_0^1 d\lambda \int d\boldsymbol{r} \frac{\partial \beta u_{\rm UV}(r,\lambda)}{\partial \lambda} g_{\rm UV}(r,\lambda). \tag{11}$$

In the language of charging technique, one may add one (marked) solute particle, U, from infinity to a given point into the $N-1$ particle solvent system solvent, V, and the intermolecular interactions between them scales until the added particle is not distinguished from the others. For the Kirkwood approach, Eq. (11), λ scales interactions of one (marked) particle with others, that is, when $\lambda = 0$, the particle is removed and when $\lambda = 1$, the particle is fully coupled to the system.

As with the Helmholtz free energy, a density dependent path can be derived. Following Watts [43] we obtain from the Gibbs-Duhem relation

$$\mu^e = \int_0^\rho d\rho' \frac{1}{\rho'}\left[\left(\frac{\partial P}{\partial \rho'}\right)_T - kT\right] \tag{12}$$

where we may use a numeric derivative of the pressure or analytic derivatives provide by Eqs. (5) or (6) (see Appendix A).

In another approach, we may use the relation $PV = G - A$ to write for a single-component system

$$\beta\mu^e = \frac{\beta A^e}{N} + \frac{\beta p}{\rho} - 1. \tag{13}$$

Various expressions for the free energy and pressure can be used here, admitting the combinations of different physical and non-physical paths. For example, we may use Eqs. (10) with (6),

$$\beta\mu^e = \int_0^\rho \frac{1}{\rho'}\Big(\frac{\beta p}{\rho'} - 1\Big) d\rho' - \frac{1}{\rho}\int_0^\rho \rho' d\rho' \int c(\boldsymbol{r},\rho') d\boldsymbol{r}, \tag{14}$$

Eqs. (10) with (5),

$$\beta\mu^e = \int_0^\rho \frac{1}{\rho'}\Big(\frac{\beta p}{\rho'} - 1\Big) d\rho' - \frac{\rho}{6}\int d\boldsymbol{r} r \frac{\partial \beta u(r)}{\partial r} g(r) \tag{15}$$

Eqs. (9) with (6),

$$\begin{aligned}\beta\mu^e = \frac{\rho}{2}\int_0^1 d\lambda \int d\boldsymbol{r} \frac{\partial \beta u(r,\lambda)}{\partial \lambda} g(r,\lambda) \\ -\frac{1}{\rho}\int_0^\rho \rho' d\rho' \int c(\boldsymbol{r},\rho') d\boldsymbol{r}'\end{aligned} \tag{16}$$

or Eqs. (9) with (5),

$$\begin{aligned}\beta\mu^e = \frac{\rho}{2}\int_0^1 d\lambda \int d\boldsymbol{r} \frac{\partial \beta u(r,\lambda)}{\partial \lambda} g(r,\lambda) \\ -\frac{\rho}{6}\int d\boldsymbol{r} r \frac{\partial \beta u(r)}{\partial r} g(r).\end{aligned} \tag{17}$$

The bridge function and thermodynamic consistency and path dependence

A closed form expression for the bridge function is not known so one must attempt to build an approximate bridge function $B(r)$ either theoretically or empirically. For the former approach, one needs to compute a series expansion for $B(r)$ in powers of the density in which each term may represent the sum of diagrams which are computed in terms of the multidimensional integrals, and so cannot be completely utilized in practice [38, 44, 45].

The latter case is technically easer than the former. However, when constructing $B(r)$, one should take care to preserve the thermodynamic consistency, which is the property that state variables are path independent and do not depend on the path taken in the physical or mathematical sense. There are several types of thermodynamic consistency conditions, for example [46–48]: virial and compressibility pressure,

$$p^v = p^c, \tag{18}$$

internal energy and pressure,

$$\rho^2 \left(\frac{\partial \beta E/N}{\partial \rho}\right)_T = -T \left(\frac{\partial \beta p}{\partial T}\right)_\rho, \tag{19}$$

virial pressure and free energy,

$$\beta\mu^e = \frac{\beta A^e}{N} + \frac{\beta p^v}{\rho} - 1, \tag{20}$$

and Gibbs-Duhem

$$\left(\frac{d\mu}{dp}\right)_T = \frac{1}{\rho}. \tag{21}$$

These conditions can either be directly tested for or explicitly enforced e.g., through the introduction free parameters in the closure relation that can be tuned. In this work, we enforce Eq. (18) and test the other three relations. Internal energy and pressure consistency is checked through numerical and analytic derivatives of Eqs. (1), (8), and (5), while virial pressure and energy consistency is checked with Eq. (15). The Gibbs-Duhem relation is checked with Eqs. (A2) and (A1); however, if $\left(\frac{dp^v}{d\rho}\right)_T = \left(\frac{dp^c}{d\rho}\right)_T$ is not satisfied, these three equations are not equivalent. For example, HNC exhibits Gibbs-Duhem consistency when the viral pressure is used, Eq. (A2), but not if the compressibility is used, Eq. (12).

In addition, path independence is required for the chemical potential and Helmholtz free energy. For example, Eqs. (9) and (11) should not depend on how the coupling parameter is included. To handle this path-dependence issue, Kast has given the sufficient conditions for constructing bridge function $B(r)$, which implies path-independence [24]. Kast found that path independence is implied if the variational parameter

$$q = \frac{\frac{\partial B}{\partial \gamma} - \frac{\partial B}{\partial c} + 1}{\frac{\partial B}{\partial u} - \beta} \tag{22}$$

is independent of the spatial coordinates and λ (see also Appendix B). Therefore, any function $B(\gamma - \beta u)$, $B(c + \beta u)$, $B(h, \gamma - \beta u)$, $B(h, c + \beta u)$ and $B(h)$ has guaranteed path independence in RISM theory and, therefore, OZ theory. Importantly, renormalized bridge functions, where only the long-range or short-range part of the potential is used, do not satisfy this condition. Nor do functions that are a function of γ, $B(\gamma)$. Such bridge functions may be path-independent but this is difficult to prove and must be done on an individual basis.

A free energy and pressure path-independent closure

In this work we employ the virial and compressibility pressure consistency, commonly known as "pressure consistency", and free energy consistency. Among mentioned bridge approximations, none of them satisfy both thermodynamic conditions we considered here. The VM, ZH, RY and MV approximations satisfy pressure consistency while the HNC, PSE-n, and KH approximations satisfy the path-independence. Therefore, we propose a new approximation for $B(r)$ which satisfies both the thermodynamic consistency and path-independence conditions,

$$B(r) = ac(r) + \sum_i b_i h^i(r), \quad i = 1, 2, 3, \ldots \tag{23}$$

where a and b are free parameters, which may be selected to satisfy other consistency conditions. Although this proposed equation explicitly includes the direct correlation function, it satisfies the requirements for path-independence since Eq. (22) is constant and independent of spatial coordinate/coupling parameter. Details are given in Appendix B. For simplicity, in the numerical part of this work we employ only the first order expansion of the proposed bridge function,

$$B = ac(r) + bh(r). \tag{24}$$

In order to simplify the computational work required, it is advantageous to have an analytical, closed-form formula to evaluate the excess free energy or chemical potential. Using the Kirkwood charging formula, Eq. (9), and Eq. (23) we can obtain an analytic formula for evaluation of the excess Helmholtz free energy (see Appendix C):

$$\frac{\beta A^e}{N} = \frac{\beta A^{\mathrm{HNC}}}{N} + \frac{\rho}{2}\int d\boldsymbol{r} g B - \frac{a}{2}\frac{1}{8\pi^3}\int d\boldsymbol{k}\Big[\hat{h} - \frac{1}{\rho} \times \ln|1 + \rho\hat{h}|\Big] - \frac{\rho}{2}\int \sum_i \frac{b_i}{i+1} h^{i+1} d\mathbf{r}, \ (i = 1, 2, \ldots) \tag{25}$$

Here is $\beta A^{\mathrm{HNC}}/N$ is the HNC-type expression for the excess Helmholtz free energy with appropriate bridge function $B(r)$,

$$\frac{\beta A^{\mathrm{HNC}}}{N} = \frac{\rho}{2}\int d\boldsymbol{r}\Big(\frac{1}{2}h^2 - c\Big) + \frac{1}{2}\frac{1}{8\pi^3}\int d\boldsymbol{k}\Big[\hat{c} + \frac{1}{\rho}\ln|1 - \rho\hat{c}|\Big]. \tag{26}$$

Using similar approach (see Appendix C) we can obtain an approximate analytical expression for the VM closure

$$\frac{\beta A^e}{N} = \frac{\beta A^{\mathrm{HNC}}}{N} + \frac{\rho}{2}\int d\boldsymbol{r} g B + \frac{\rho}{4}\frac{1}{8\pi^3}\int d\boldsymbol{k}\hat{h} \times \int_0^1 d\nu \left(\frac{\phi\left(\rho\nu^2\hat{h}^2/\left(1+\rho\nu\hat{h}\right)\right)^2}{1 + \alpha\rho\nu^2\hat{h}^2/\left(1+\rho\nu\hat{h}\right)}\right). \tag{27}$$

where ν is a coupling parameter.

For excess chemical potential we have derived a formula with a proposed bridge function (see Appendix B and Appendix C):

$$\beta\mu^{e} = \beta\mu^{\mathrm{HNC}} + \rho\int d\boldsymbol{r} gB - \rho\int d\boldsymbol{r}\Big[\frac{1}{2}ahc + (\sum_{i=1}\frac{b_i}{i+1}h^{i+1})\Big], \tag{28}$$

where $\beta\mu^{\mathrm{HNC}}$ is the HNC-type expression for the excess chemical potential with appropriate bridge function $B(r)$ [38, 49],

$$\beta\mu^{\mathrm{HNC}} = \rho\int d\boldsymbol{r}\Big(\frac{1}{2}h^2 - c - \frac{1}{2}hc\Big). \tag{29}$$

We note that terms beyond $\beta\mu^{\mathrm{HNC}}$ in (28) resemble partial molar volume corrections that have been used extensively in for 3D-RISM and MDFT (see Appendix D).

The VM closure has no known closed-form, analytic expression for the excess chemical potential. Instead, we will employ a commonly used approximate closed expression [21, 50–53],

$$\beta\mu^{e} \approx \beta\mu^{\mathrm{HNC}} + \rho\int d\boldsymbol{r}\Big(B + \frac{2h}{3}B\Big). \tag{30}$$

With Eqs. (25) to (30) the excess Helmholtz free energy and chemical potential can be computed using only a single state at the given temperature and density.

As one would expect, setting $B = 0$ in the derived expressions for the HFE and chemical potential leads directly to expressions in the HNC approximation, Eq. (26). We note that for the excess free energy similar expressions to formula (27) had been given by Kiselyov and Martynov [21], but for the PY and MS approximations.

III. NUMERICAL PROCEDURE

In this work we consider a single-component fluid whose an interparticle potential is give by the Lennard-Jones potential

$$u(r) = 4\epsilon\left(\Big(\frac{\sigma}{r}\Big)^{12} - \Big(\frac{\sigma}{r}\Big)^{6}\right), \tag{31}$$

where σ and ϵ are the size and energy parameters of the LJ potential, respectively. For all calculations we use reduced units, in which σ and ϵ are the base units for length and energy. This gives the reduced number density, $\rho^* = \rho\sigma^3$, temperature $T^* = k_{\mathrm{B}}T/\epsilon$, and pressure, $p^* = p\sigma^3/\epsilon$.

Even when the free energy should be a path-independent property, the details of how the coupling constant is included in the potential energy are numerically important, as a simple linear coupling, $u\,(r,\lambda) = \lambda u\,(r)$, leads to large numerical errors. For this reason, a shifted and scaled LJ potential may be used, such as [54]

$$u(r,\lambda) = 4\lambda\epsilon\Big[\Big(\frac{\sigma^2}{r^2+(1-\lambda)s}\Big)^{6} - \Big(\frac{\sigma^2}{r^2+(1-\lambda)s}\Big)^{3}\Big] \tag{32}$$

where $s > 0$ is an arbitrary constant. In this approach, for each different value of λ from 0 to 1, a new $g(r,\lambda)$ is computed. Numerically computing the integral in Eq. (9) then requires solving the OZ equation at different λ. Depending on the precision required, this can be computation onerous.

An in-house MATLAB [55] code was developed to solve the OZ equation, Eq. (1), using HNC, VM, and Eq. (24) bridge approximations to obtain thermodynamic properties of the LJ fluid using the theoretical formulations described in the preceding sections. A simple Picard iterative method was applied and the numerical tolerance for the root mean squared residual of the direct correlation functions during successive iterations was set at 10^{-10}. All calculations were performed with the same number of grid points, $N = 8192$, and length parameter, $L = 32\sigma$. Thermodynamic quantities were computed for $T^* = 1.5, 2.74$, and 5 and $\rho\sigma^3 = 0.1$ to 1.1 in increments of 0.1.

At each temperature and pressure reported, pressure consistency was enforced by optimizing coefficients (a, b) in Eq. (23) and (ϕ, α) in Eq. (4) to satisfy the consistency condition. The pressure consistency equation was converged to $|p^v - p^c| \leq 10^{-6}$ using the 'fminsearch' multidimensional unconstrained nonlinear minimization routine of MATLAB. This required calculating the pressure from the virial and compressibility routes for each set of coefficients proposed by the minimizer. For the virial pressure, Eq. (5) was use directly. To calculated the compressibility pressure, Eq. (7) was employed where the trial coefficients were fixed for all intermediate densities, ρ', in the integral. HNC was excluded from pressure consistency enforcement since it has no adjustable parameters.

Numerical calculations of the pressure, free energy, and chemical potential used the mid-point integration with step sizes $d\lambda = 0.005$ and $d\rho' = 0.025$ for the Kirkwood charging and thermodynamic integration formulas, respectively. Bridge function coefficients were held constant for each of these calculations. For Eq. (32), $s = 0.5$ was used.

IV. RESULTS

Pressure consistency

In Table I we compare pressures obtained from HNC, VM, and Eq. (24) bridge approximations for the LJ potential at $\rho\sigma^3 = 0.9$ and $T^* = 1.5, 2.74$

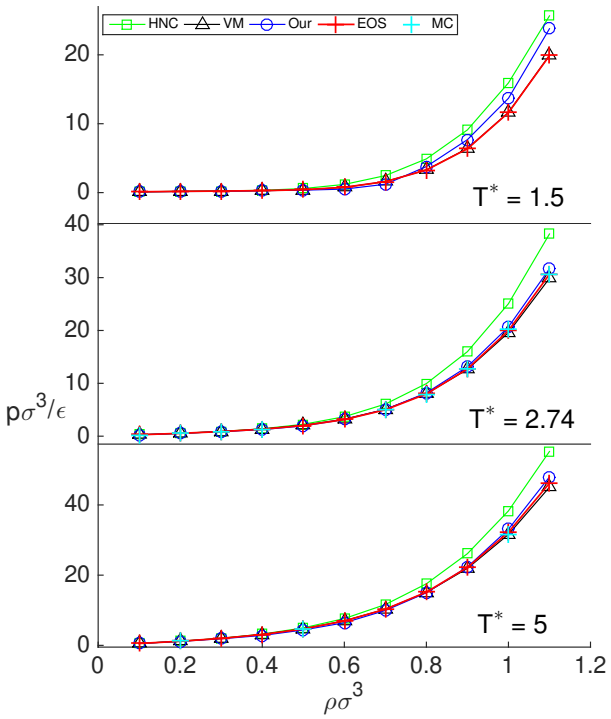

FIG. 1. Absolute pressure, $p\sigma^3/\epsilon$, as a function of density, $\rho\sigma^3$. Green, black and blue lines are from the HNC, VM and Eq. (24) bridge corrections respectively. Red crosses are from the equations of state in [35]. Cyan crosses are available MC data from [33] and [34] for $T^* = 2.74$ and 5.

and 5. As expected, both VM and Eq. (24) show virial-compressibility consistency while HNC does not. Furthermore, while both VM and (24) are within a few percent of MC and EOS data [33–35] and each other at $T^* = 2.74$ and 5, HNC values differ considerably at all temperatures. At $T^* = 1.5$, Eq. (24) is still an improvement over HNC but has increased relative error.

We note that if we use $dp^v = dp^c$ consistency instead, the obtained numerical values for both pressures would be close, but inconsistent. For example, for the LJ potential at $T^* = 2.74$ and $\rho^* = 0.9$, the VM approximation gives $p^v\sigma^3/\epsilon = 12.70$ and $p^c\sigma^3/\epsilon = 13.05$ while our closure gives $p^v\sigma^3/\epsilon = 12.94$ and $p^c\sigma^3/\epsilon = 13.92$. Therefore, we did not employ the $dp^v = dp^c$ consistency in this work.

As seen in Figure 1, the pressure for all three models is in good agreement with EOS data at low densities, regardless of temperature. HNC, however, diverges from the EOS as the density increases, always overestimating the pressure, while VM stays within a few percent. Eq. (24) also behaves like VM for $T^* = 2.74$ and 5, tracking the EOS pressure within a few percent. However, at $T^* = 1.5$, also predicts excessively high pressures at high densities.

Figure 2 shows optimized values of coefficients (a, b) of

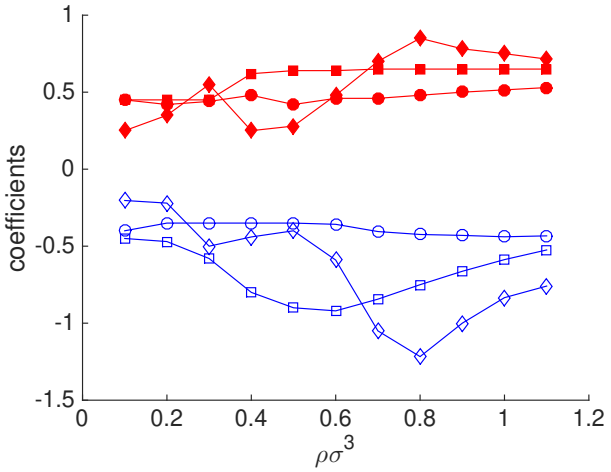

FIG. 2. Coefficients a (red, filled) and b (blue, unfilled) for Eq. (24) vs $\rho\sigma^3$ at $T^* = 1.5$ (diamonds), 2.74 (squares) and 5 (circles).

Eq. (23) vs $\rho\sigma^3$, which are obtained by enforcing viral and compressibility pressure consistency, Eq. (18). As seen here, the coefficients have both a temperature and pressure dependence though it appears to be diminished as density increases.

Energy-pressure consistency

Table II shows the consistency of pressure and internal energy through density and temperature derivatives, as given in Eq. (19). As the virial pressure is used, both HNC and Eq. (24) show consistency while VM does not. If the pressure was calculated from the compressibility route, the results for Eq. (24) would be unaffected but HNC would fail to show consistency.

Chemical potential and Helmholtz free energy

To test the path independence of our new closure, we calculated the excess Helmholtz free energy A^e/ϵ using the Kirkwood charging formula Eq. (9), density integration Eq. (10) and the respective analytical formulas, Eqs. (25), (26), and (27). In Table III we show the values for A^e/ϵ at $T^* = 1.5, 2.74$ and 5 for $\rho\sigma^3 = 0.9$. As expected, results from HNC and (24) show no path dependence. The VM results, however, are path-dependent, with the Kirkwood and density integration formulas giving different, but close, values. The analytical expression for VM is not expected to be consistent with the numerical values, as it is an approximation, though it gives reasonable values. In contrast to the calculated pressure, Eq. (24) has the best agreement with EOS at the values at low temperatures while VM performs better at high temperatures. HNC

TABLE I. The pressure, $p\sigma^3/\epsilon$, from virial and compressibility routes for the LJ potential at $\rho\sigma^3 = 0.9$.

	$T^* = 1.5$			$T^* = 2.74$			$T^* = 5$		
	HNC	VM	Eq. (24)	HNC	VM	Eq. (24)	HNC	VM	Eq. (24)
Virial	9.104	6.421	7.688	15.99	12.64	13.15	26.12	21.92	22.32
Compressibility	3.781	6.421	7.688	9.415	12.64	13.15	18.12	21.92	22.32
MC						12.68[33]			
EOS			6.365[35]			12.72[35]			22.19[35]

TABLE II. Internal energy-pressure consistency for the LJ potential at $\rho\sigma^3 = 0.9$.

	$T^* = 2.74$			$T^* = 5$		
	HNC	VM	Eq. (24)	HNC	VM	Eq. (24)
$\rho^2 \left(\frac{\partial \beta E/N}{\partial \rho}\right)_T$	0.910	0.120	0.550	1.267	0.563	0.949
$-T \left(\frac{\partial \beta p}{\partial T}\right)_\rho$	0.910	0.099	0.550	1.267	0.675	0.949

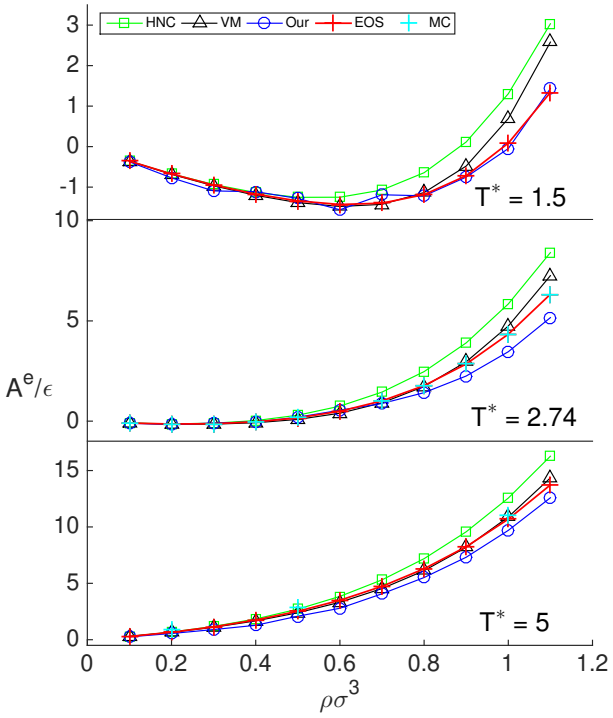

FIG. 3. Helmholtz free energy per particle, A^e/ϵ, as a function of density, $\rho\sigma^3$. Green, black and blue lines are from the HNC, VM and Eq. (24) bridge corrections respectively. Red crosses are from the equations of state in [35]. Cyan crosses are MC simulation data taken from [33] and [34] for $T^* = 2.74$ and 5.

over estimates the Helmholtz free energy in all cases and has the largest relative error.

Results for the excess Helmholtz free energy over a range of densities are shown in Figure 3 for temperatures $T^* = 2.74$ and 5. HNC overestimates the free energy while the new bridge approximation tends to

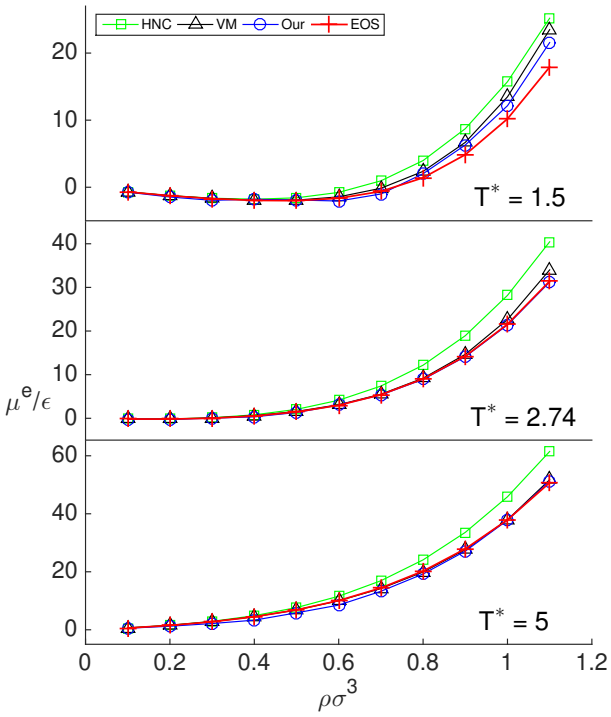

FIG. 4. Excess chemical potential, μ^e/ϵ, as a function of density, $\rho\sigma^3$. Green, black and blue lines are from the HNC, VM and Eq. (24) bridge corrections respectively. Red crosses are from the equations of state in [35].

underestimate the free energy at higher densities. This is most apparent at $T^* = 2.74$ but the same behavior is also observed at $T^* = 5$. Only values for the analytical expression for the VM free energy are shown, but these are in good agreement with simulation at all temperatures and densities.

Several paths for the excess chemical potential are compared in Table IV for all three closure approximations. We can see that for all closures the agreement of the various numerical approaches with the analytic expression depends on which path was used. All closures display inconsistency between the virial and compressibility expressions for Gibbs-Duhem, Eq. (12). This is due to inconsistency in the density derivative of the pressure, which all of these closures exhibit. We note that the virial expression for Gibbs-Duhem is consistent

TABLE III. The excess Helmholtz free energy, A^e/ϵ, per particle for the LJ potential at $\rho\sigma^3 = 0.9$.

	$T^* = 1.5$			$T^* = 2.74$			$T^* = 5$		
	HNC	VM	Eq. (24)	HNC	VM	Eq. (24)	HNC	VM	Eq. (24)
Kirkwood Eq. (9)	0.115	-0.600	-0.752	3.904	2.630	2.251	9.570	8.009	7.315
TI density Eq. (10)	0.115	-0.951	-0.752	3.904	2.700	2.251	9.570	8.127	7.315
Analytic Eq. (26, Eq. (25), Eq. (27))	0.115	-0.493	-0.752	3.904	2.961	2.251	9.570	8.194	7.315
MC						2.850[33]			
EOS		-0.720[35]				2.850[35]			8.248[35]

TABLE IV. The excess chemical potential μ^e/ϵ for the LJ potential at $\rho\sigma^3 = 0.9$.

	$T^* = 1.5$			$T^* = 2.74$			$T^* = 5$		
	HNC	VM	Eq. (24)	HNC	VM	Eq. (24)	HNC	VM	Eq. (24)
Gibbs-Duhem									
Compressibility Eq. (A2)	1.479	5.505	6.693	9.811	14.52	13.77	22.32	27.80	27.33
Virial Eq. (A1)	8.726	4.680	6.292	18.93	14.00	14.13	33.59	27.49	27.12
Kirkwood-compressibility Eq. (16)	2.816	5.035	6.291	11.62	13.93	14.13	24.70	27.38	27.12
Kirkwood-virial Eq. (17)	8.730	5.035	6.292	18.93	13.93	14.13	33.59	27.37	27.12
Free energy and pressure									
TI density-compressibility Eq. (14)	2.816	4.684	6.291	11.62	14.00	14.13	24.70	27.50	27.12
TI density virial Eq. (15)	8.730	4.684	6.292	18.93	14.00	14.13	33.59	27.49	27.12
Analytic (Eqs. (29, (30), (28))									
	8.730	5.517	6.293	18.93	14.65	14.13	33.59	27.60	27.12
EOS [35]			4.852			14.24			27.90

with the analytic expression for both HNC and Eq. (24).

Consistency for different thermodynamic routes for the free energy-pressure equation, Eq. (13), naturally depends on the consistency of the free energy and pressure of the respective closures. HNC has free energy consistency but not pressure consistency – as long as the virial path is used Gibbs-Duhem, free energy and pressure, and the analytic expressions all agree. Conversely, VM has pressure consistency but not free energy consistency, so Kirkwood and density paths to the free energy and chemical potential do not agree. However, density integration is consistent with the virial Gibbs-Duhem expression. Because Eq. (24) exhibits both free energy and pressure consistency, all routes agree, except for the compressibility Gibbs-Duhem expression.

VM and Eq. (24) have similar accuracy for the chemical potential over a range of temperatures and compare well to the EOS, as shown in Figure 4. Again, HNC over-estimates the MC data and is significantly higher than VM and Eq. (24). Analytic expressions were used for all three closures. Overall, Eq. (24) has better agreement with the excess chemical potential than it does with the Helmhotz free energy (Figure 3) especially at high temperatures and is similar to that observed for the pressure (Figure 1).

V. DISCUSSION

Thermodynamically consistent behavior is an essential property for a successful theory of liquids. The primary result of this work is the development of a closure for the OZ equation that has both pressure and free energy consistency. While pressure consistent and free energy path independent closures have been developed before, this is the first time that a single closure has demonstrated both.

A. Thermodynamic Consistency

To examine how satisfying both types of thermodynamic consistency can improve the predictive power of the OZ equation, we compared our results against VM and HNC closures. These alternately satisfy virial-compressibility pressure consistency (VM) or path independence for the free energy respectively (HNC) but not both. All other closures that we are aware of like-wise either only satisfy virial-compressibility pressure consistency or path independence for the chemical potential and free energy. As expected, enforcing pressure consistency improves predictions of the pressure from VM and Eq. (24) compared to HNC, particularly at high temperature and density.

We have more routes to the free energy and chemical potential, which allows us to examine in greater detail the implications of thermodynamic consistency or lack thereof. Because Eq. (24) satisfies the Kast criteria [24] (see Appendix B) and pressure consistency is enforced, all routes to the free energy and chemical potential provide consistent results except for the Gibbs-Duhem expression using the compressibility, Eq. (A2), which we discuss

below. HNC does have internal energy-virial consistency but not pressure consistency, so any expression that uses the compressibility route is inconsistent but viral and Kirkwood results are consistent, which includes the analytic expressions. The VM closure only exhibits pressure consistency, so analytic expressions are simply approximations. Numeric results may agree with each other but only when the only difference is whether the pressure is calculated from the viral or compressibility route.

To achieve consistency for all routes to the chemical potential tested here it is necessary to have consistency of the density derivative of the pressure, $\left(\frac{dp^v}{d\rho}\right)_T = \left(\frac{dp^c}{d\rho}\right)_T$, while satisfying pressure consistency. None of the three closures satisfy this, as is demonstrated by the results for the Gibbs-Duhem expression for the chemical potential, Table IV. For this additional consistency, it is necessary that the free parameters in the bridge be independent of density.

An additional consequence of free energy path independence is that we were able to derive analytical, closed form formulas for the excess free energy and excess chemical potential for our new closure. This allows the excess free energy and excess chemical potential to be computed without the Kirkwood charging or any other numerical form of thermodynamic integration. Indeed, we find that these formulas are completely consistent with the various numerical paths we have tested for Eq. (25). This is in contrast to the approximate formulas for VM, which are in poor agreement with various numerical results.

B. Partial molar volume correction

Some physical insight to the success of our new closure can be gained by comparing it to the various partial molar volume based corrections that have been proposed for 3D-RISM theory and molecular density functional theory (MDFT) [28–31]. Upon close inspection of our analytic formula for the excess chemical potential, Eq. (D1), and the Universal Correction applied to HNC, Eq. (D5), we find that though the coefficients are slightly different, the leading terms are nearly identical. PMV corrections used in 3D-RISM and MDFT work by compensating for mechanical work (pressure-volume) required to introduce a solute. In the case of HNC-like closures, the pressure is much too high, leading to chemical potentials that are also much too large. By enforcing pressure consistency of our proposed closure, the pressure is directly tuned and accounted for at the closure level without fitting to external data.

PMV corrections have been used successfully for water (e.g., [29–31, 56–58]) and other solvents (e.g., [59–62]). Because room temperature and atmospheric pressure are typical physical conditions for solvated biological and non-biological systems, we anticipate that this closure will work well where PMV corrections have been used before. For example, simulations of water are commonly performed at $T = 298.15\,K$ and $\rho = 997\,kg/m^3$ or $T^* = 3.82$ and $\rho^* = 1.06$ using the SPC/E model [63]. These conditions correspond to the highest temperatures and densities we tested, where we observed pressures and chemical potentials in good agreement with the equation of state. Non-polar solvents, such as cyclohexane, have similar reduced temperatures but lower densities than water for similar calculations. Indeed, we expect that this closure will perform well for typical solvation free energy calculations for which PMV corrections have been used in the past.

VI. CONCLUSION

In this work we have proposed a new closure equation, Eq. (23), for the Ornstein-Zernike equation that satisfies both virial-compressibility pressure consistency and path independence for the chemical potential and free energy. As a consequence, this closure also exhibits internal energy-pressure, free energy-pressure, and Gibbs-Duhem consistency. This consistency was demonstrated by calculating solutions to the Ornstein-Zernike equation with just the first order of our new closure, Eq. (24), for the Lennard-Jones potential at thermodynamic parameters $T^* = 1.5, 2.74$ and 5, and $\rho\sigma^3 = 0.1$ to 1.1. In addition, we were able to derive closed form expressions for the free energy and chemical potential. We anticipate that this closure will be particularly useful for calculations of common solvents in 3D-RISM and molecular CDFT calculations where PMV corrections are currently used.

ACKNOWLEDGEMENT

This material is based upon work supported by the National Science Foundation (NSF) under Grant No. (1566638) and a Cottrell Scholar Award from the Research Corporation for Science Advancement (RCSA).

Appendix A: Density derivative path to the chemical potential

Following [43], when we hold the temperature constant, starting from the thermodynamic identity

$$dG = V\,dp - S\,dT,$$

we have

$$\left(\frac{\partial G}{\partial p}\right)_T = V$$
$$\left(\frac{\partial \mu}{\partial p}\right)_T = \rho^{-1}$$
$$\left(\frac{\partial \mu}{\partial \rho}\right)_T \left(\frac{\partial \rho}{\partial p}\right)_T = \rho^{-1}$$
$$\left(\frac{\partial \mu^e}{\partial \rho}\right)_T + \left(\frac{\partial \mu^i}{\partial \rho}\right)_T = \rho^{-1}\left[\left(\frac{\partial p^e}{\partial \rho}\right)_T + \left(\frac{\partial P^i}{\partial \rho}\right)_T\right].$$

In the second step we have the Gibbs-Duhem relation and in the last step we have split the chemical potential into excess, e, and ideal, i, contributions. For the ideal contribution on the right hand side we have

$$\left(\frac{\partial p^i}{\partial \rho}\right)_T = \frac{\partial}{\partial \rho}\rho kT = kT$$

where we have used the ideal gas law. For the excess chemical potential, we then have

$$\left(\frac{\partial \mu^e}{\partial \rho}\right)_T = \rho^{-1}\left[\left(\frac{\partial p}{\partial \rho}\right)_T - kT\right]$$
$$\mu^e = \int_0^\rho d\rho' \frac{1}{\rho'}\left[\left(\frac{\partial p}{\partial \rho'}\right)_T - kT\right]$$

We may use either Eq. (5) or Eq. (6) for the derivative of the pressure. Using Eq. (5), we have

$$\begin{aligned}\mu^e &= \int_0^\rho d\rho' \frac{1}{\rho'}\Big[kT\Big(1 - 2\frac{\rho'}{6}\int d\boldsymbol{r} r \frac{\partial \beta u(r)}{\partial r} g(r) \\ &\quad - \frac{\rho'^2}{6}\int d\boldsymbol{r} r \frac{\partial \beta u(r)}{\partial r}\frac{\partial g(r)}{\partial \rho'}\Big) - kT\Big] \\ &= -kT\int_0^\rho d\rho'\Big[\frac{1}{3}\int d\boldsymbol{r} r \frac{\partial \beta u(r)}{\partial r} g(r) \\ &\quad + \frac{\rho'}{6}\int d\boldsymbol{r} r \frac{\partial \beta u(r)}{\partial r}\frac{\partial g(r)}{\partial \rho'}\Big]. \end{aligned} \tag{A1}$$

Using Eq. (6) we have

$$\begin{aligned}\mu^e &= \int_0^\rho d\rho' \frac{1}{\rho'}\left[kT\left(1 - \rho'\int c(r,\rho') d\boldsymbol{r}\right) - kT\right] \\ &= -kT\int_0^\rho d\rho' \int c(r,\rho') d\boldsymbol{r} \end{aligned} \tag{A2}$$

which is the result obtained by [43].

Appendix B: Free energy path independence and closed-form chemical potential

Kast [24] uses a variational approach to obtain a constrained formula for the excess chemical potential

$$\mu^e = \int_0^1 \int \rho(h+1)\frac{\partial u}{\partial \lambda} + pP + vV \, d\mathbf{r}\, d\lambda + \frac{q}{(2\pi)^3}\int_0^1 \int Q \, d\mathbf{k} \tag{B1}$$

where, in the general case,

$$\begin{aligned} P &= \exp(-\beta u + \gamma + B) - h - 1, \\ V &= h - c - \gamma, \\ Q &= \rho\hat{c}\frac{\partial \hat{c}}{\partial \lambda}\left(1 + \frac{\rho\hat{c}}{1-\rho\hat{c}}\right) - \frac{\partial \hat{c}}{\partial \lambda}\rho\hat{h} \end{aligned}$$

and p, v, and q are variational parameters to be solved for. For path-independence to be satisfied, the functional derivatives of Eq. (B1) with respect to h, c, γ, and u must be zero:

$$\frac{\partial \mu^e}{\partial h} = \rho\frac{\partial u}{\partial \lambda} + p\left[\frac{\partial B}{\partial h}(h+1) - 1\right] - q\rho\frac{\partial c}{\partial \lambda} + v = 0, \tag{B2}$$

$$\frac{\partial \mu^e}{\partial c} = p\frac{\partial B}{\partial c}(h+1) + q\rho\frac{\partial h}{\partial \lambda} - v = 0, \tag{B3}$$

$$\frac{\partial \mu^e}{\partial \gamma} = p\left(\frac{\partial B}{\partial \gamma} + 1\right)(h+1) - v = 0, \tag{B4}$$

$$\frac{\partial \mu^e}{\partial u} = p\left(\frac{\partial B}{\partial u} - \beta\right)(h+1) - \rho\frac{\partial h}{\partial \lambda} = 0. \tag{B5}$$

This system of equations is then solved for p, v and q, giving

$$p = \rho\frac{\partial h}{\partial \lambda}\frac{1}{\left(\frac{\partial B}{\partial u} - \beta\right)(h+1)}, \tag{B6}$$

$$v = \rho\frac{\partial h}{\partial \lambda}\frac{\frac{\partial B}{\partial \gamma} + 1}{\frac{\partial B}{\partial u} - \beta}, \tag{B7}$$

$$q = \frac{\frac{\partial B}{\partial \gamma} - \frac{\partial B}{\partial c} + 1}{\frac{\partial B}{\partial u} - \beta}. \tag{B8}$$

For a closure with bridge approximation given by Eq. (23) we may obtain

$$\begin{aligned} p &= -\beta^{-1}(h+1)^{-1}\frac{\partial h}{\partial \lambda} \qquad v = -\beta^{-1}\rho\frac{\partial h}{\partial \lambda}, \\ q &= -\beta^{-1}(1-a). \end{aligned} \tag{B9}$$

From the equation for q in Eq. (B9) it is seen that the proposed bridge approximation Eq. (23) has satisfied this path independence condition.

Combining Eqs. (B2) with (11) and p, v and q we have

$$\begin{aligned}\mu^e = \mu^{\mathrm{HNC}} &- \rho\int_0^1 \int d\mathbf{r}\, d\lambda \frac{1}{\left(\frac{\partial B}{\partial u} - \beta\right)} \\ &\left\{\frac{\partial h}{\partial \lambda}(h+1)\left[\frac{\partial B}{\partial h} + \frac{\partial B}{\partial \gamma}\right]\right. \\ &\left. - \frac{\partial c}{\partial \lambda}(h+1)\left(\frac{\partial B}{\partial t} - \frac{\partial B}{\partial c}\right)\right\}. \end{aligned} \tag{B10}$$

It is straightforward to extend this to multicomponent 1D- or 3D-RISM cases.

For the specific case of Eq. (23) we have

$$\frac{\partial B}{\partial u}=0, \qquad \frac{\partial B}{\partial \gamma}=0,$$
$$\frac{\partial B}{\partial c}=a, \qquad \frac{\partial B}{\partial h}=\sum_{i=1} i b_i h^{i-1},$$

and Eq. (B10) reduces to

$$\mu^e=\mu^{\rm HNC}-\frac{\rho}{\beta}\int d\mathbf{r} \left\{b_1 h+\sum_{i=2}\left(b_i+b_{i-1}\left(1-\frac{1}{i}\right)\right)h^i - \frac{1}{2}ahc+ac\right\} \tag{B11}$$

Appendix C: Closed form expressions for free energy and chemical potential

To eliminate a derivative of $\partial u/\partial\lambda$ in the Kirkwood charging formulas, Eqs. (9) and (11), we begin with the exact expression

$$(1+h(\boldsymbol{r},\lambda))=e^{-\beta u(\boldsymbol{r},\lambda)+h(\boldsymbol{r},\lambda)-c(\boldsymbol{r},\lambda)+B(\boldsymbol{r},\lambda)}. \tag{C1}$$

Taking the derivative of both sides we arrive at

$$\beta(1+h)\frac{\partial u}{\partial\lambda}=\frac{\partial}{\partial\lambda}\Big(\frac{1}{2}h^2-c+B\Big)-h\frac{\partial c}{\partial\lambda}+h\frac{\partial B}{\partial\lambda}. \tag{C2}$$

Inserting Eq. (C2) into the Kirkwood charging formula for the excess free energy, Eq. (9), we have

$$\frac{\beta A^e}{N}=\frac{\rho}{2}\int d\boldsymbol{r}\Big(\frac{1}{2}h^2-c+B\Big)-\frac{\rho}{2}\int_0^1 d\lambda\int d\boldsymbol{r}h\frac{\partial c}{\partial\lambda} +\frac{\rho}{2}\int_0^1 d\lambda\int d\boldsymbol{r}h\frac{\partial B}{\partial\lambda} \tag{C3}$$

In the second integral we need to express h in terms of c in order to integrate over λ, that is,

$$\begin{aligned}\int_0^1 d\lambda\int d\boldsymbol{r}h\frac{\partial c}{\partial\lambda}&=\int_0^1 d\nu\int d\boldsymbol{r}hc\\ &=\frac{1}{8\pi^3}\int_0^1 d\nu\int d\boldsymbol{k}\,\widehat{h(\nu c)}\,\hat{c}\\ &=\frac{1}{8\pi^3}\int_0^1 d\nu\int d\boldsymbol{k}\frac{\nu\hat{c}}{1-\rho\nu\hat{c}}\hat{c}\\ &=\frac{1}{8\pi^3}\int d\boldsymbol{k}\hat{c}^2\int_0^1 d\nu\frac{\nu}{1-\rho\nu\hat{c}}\\ &=-\frac{1}{8\pi^3}\frac{1}{\rho}\int d\boldsymbol{k}\Big[\hat{c}+\frac{1}{\rho}\ln|1-\rho\hat{c}|\Big].\end{aligned} \tag{C4}$$

Here we used $(\partial c/\partial\lambda)d\lambda=cd\nu$ and $\widehat{\nu c}=\nu\hat{c}$ and Parseval's Theorem $\int a(\boldsymbol{r})b(\boldsymbol{r})d\boldsymbol{r}=(1/8\pi^3)\int\hat{a}\hat{b}d\boldsymbol{k}$ [21].

For the third integral, we can write

$$\int\int_0^1 h\frac{\partial B}{\partial h}d\lambda d\boldsymbol{r}=\int hBd\boldsymbol{r}-\int\int_0^1 B\frac{\partial h}{\partial\lambda}d\lambda d\boldsymbol{r}. \tag{C5}$$

If we assume that $h(r,\lambda)\approx\lambda h(r)$ and use expression Eq. (23) for $B(r)$, the second integral of Eq. (C5) becomes

$$\begin{aligned}\int\int_0^1 ac\frac{\partial h}{\partial\lambda}d\lambda d\boldsymbol{r}+\sum_i b_i\int\int_0^1 h^i\frac{\partial h}{\partial\lambda}d\lambda d\boldsymbol{r}&\\ =\frac{1}{8\pi^3}\frac{a}{\rho}\int d\boldsymbol{k}\Big[\hat{h}-\frac{1}{\rho}\ln|1+\rho\hat{h}|\Big]&\\ +\int d\boldsymbol{r}\sum_i\frac{b_i}{i+1}h^{i+1}.&\end{aligned} \tag{C6}$$

Combining Eqs. (C5)-(C6), we have

$$\begin{aligned}\frac{\beta A^e}{N}=&\frac{\rho}{2}\int d\boldsymbol{r}\Big(\frac{1}{2}h^2-c\Big)\\ &+\frac{1}{2}\frac{1}{8\pi^3}\int d\boldsymbol{k}\Big[\hat{c}+\frac{1}{\rho}\ln|1-\rho\hat{c}|\Big]\\ &+\frac{\rho}{2}\int d\boldsymbol{r}gB\\ &-\frac{a}{2}\frac{1}{8\pi^3}\int d\boldsymbol{k}\Big[\hat{h}-\frac{1}{\rho}\ln|1+\rho\hat{h}|\Big]\\ &-\frac{\rho}{2}\int\sum_i\frac{b_i}{i+1}h^{i+1}d\mathbf{r}.\end{aligned} \tag{C7}$$

For the VM closure, we may follow the same procedure with the caveat that a particular coupling of λ and μ has been selected. Since the VM closure is not path independent, the result is an approximation. Proceeding with this understanding, the second integral of Eq. (C5) may become

$$\begin{aligned}\int_0^1 d\lambda\int B\frac{\partial h}{\partial\lambda}d\boldsymbol{r}&=\int_0^1 d\nu\int Bhd\boldsymbol{r}\\ &=\frac{1}{8\pi^3}\int_0^1 d\nu\int d\boldsymbol{k}\,\widehat{B(\nu h)}\,\hat{h}\\ &=-\frac{1}{2}\frac{1}{8\pi^3}\int d\boldsymbol{k}\hat{h}\int_0^1 d\nu\\ &\quad\times\frac{\phi\left(\rho\nu^2\hat{h}^2/(1+\rho\nu\hat{h})\right)^2}{1+\alpha\nu^2\hat{h}^2/(1+\rho\nu\hat{h})}.\end{aligned} \tag{C8}$$

Then combining Eqs. (C5) and (C8) we have

$$\begin{aligned}\frac{\beta A^e}{N}=&\frac{\rho}{2}\int d\boldsymbol{r}\Big(\frac{1}{2}h^2-c\Big)\\ &+\frac{1}{2}\frac{1}{8\pi^3}\int d\boldsymbol{k}\Big[\hat{c}+\frac{1}{\rho}\ln|1-\rho\hat{c}|\Big]\\ &+\frac{\rho}{2}\int d\boldsymbol{r}gB\\ &+\frac{\rho}{4}\frac{1}{8\pi^3}\int d\boldsymbol{k}\hat{h}\int_0^1 d\nu\frac{\phi(\rho\nu^2\hat{h}^2/(1+\rho\nu\hat{h}))^2}{(1+\alpha\nu^2\hat{h}^2/(1+\rho\nu\hat{h}))}.\end{aligned} \tag{C9}$$

For the excess chemical potential $\beta\mu^e$, from Eqs. (11) and (C2), we can write

$$\begin{aligned}\beta\mu^e = \rho\int d\boldsymbol{r}\Big(\frac{1}{2}h_{\rm UV}^2 - c_{\rm UV} + B_{\rm UV}\Big)\\ - \rho\int_0^1 d\lambda\int d\boldsymbol{r}h_{\rm UV}\frac{\partial c_{\rm UV}}{\partial\lambda}\\ + \rho\int_0^1 d\lambda\int d\boldsymbol{r}h_{\rm UV}\frac{\partial B_{\rm UV}}{\partial\lambda}.\end{aligned} \tag{C10}$$

Where UV denotes correlation functions between a marked solute particle, U, and the bulk solvent liquid, V. While this looks almost identical to Eq. (C3), in this case λ scales the interaction between the single marked particle and the liquid rather than all of the interactions in the liquid. The OZ equation for the solute particle is then [64]

$$h^{\rm UV}(r) = c^{\rm UV}(r) + \rho\int c^{\rm UV}(|\boldsymbol{r}-\boldsymbol{r}')h^{\rm VV}(\boldsymbol{r}')d\boldsymbol{r}'.$$

Because $h^{\rm VV}(\boldsymbol{r})$ does not depend on λ, we may choose that $c(r,\lambda) = \lambda c(r)$, which leads to

$$\begin{aligned}\beta\mu^e = \rho\int d\boldsymbol{r}\Big(\frac{1}{2}h^2 - c - \frac{1}{2}hc\Big) + \rho\int d\boldsymbol{r}gB\\ - \rho\int d\boldsymbol{r}\Big[\frac{1}{2}ahc + (\sum_i\frac{b_i}{i+1}h^{i+1})\Big]\end{aligned} \tag{C11}$$

In evaluation of the excess chemical potential $\beta\mu^e$ for the VM approximation, the second integral of Eq. (C5) becomes

$$\int B\frac{\partial h}{\partial\lambda}d\lambda d\boldsymbol{r} = \int B'hd\boldsymbol{r} \approx \int\frac{B}{3}hd\boldsymbol{r}. \tag{C12}$$

Here B' denotes the series of integrated bridge diagrams with the h bond removed [21]. Combining Eqs. (C5) and (C12), and inserting them in Eq. (C11), we have

$$\beta\mu^e = \rho\int d\boldsymbol{r}\Big(\frac{1}{2}h^2 - c - \frac{1}{2}hc\Big) + \rho\int d\boldsymbol{r}(B + \frac{2h}{3}B). \tag{C13}$$

Appendix D: Connection to PMV corrections

The analytic expression for the excess chemical potential, Eq. (28), bears a strong resemblance to PMV corrections that have been used with 3D-RISM theory and molecular density functional theory [28–31]. To see the connection, we first expand Eq. (28) to the form

$$\begin{aligned}\beta\mu^e = \beta\Big\{\mu^{\rm HNC} + a\rho\int d\boldsymbol{r}c + b_1\rho\int d\boldsymbol{r}h\\ + \frac{a}{2}\rho\int d\boldsymbol{r}hc - \sum_{i=2}\left(b_i + b_{i-1}\left(1-\frac{1}{i}\right)\right)\rho\int d\boldsymbol{r}h^i\Big\}\end{aligned} \tag{D1}$$

The most general of the PMV corrections is the Universal Correction [28], which can be applied to the HNC expression as

$$\beta\mu^{\rm UC} = \beta\left\{\mu^{\rm HNC} + a\rho v + b\right\}, \tag{D2}$$

where a and b are parameters fit to experiment and v is the PMV,

$$v = k_{\rm B}T\chi_T\left(1 - \rho\int c\left(\mathbf{r}\right)d\mathbf{r}\right). \tag{D3}$$

It is useful to expand v using an alternate expression for the isothermal compressibility [36, 37, 65],

$$\chi_T = \frac{\beta}{\rho} + \beta\int h\,d\mathbf{r}. \tag{D4}$$

Combining (D2), (D3), and (D4), we have

$$\begin{aligned}\beta\mu^{\rm UC} = \beta\Big\{\mu^{\rm HNC} + a\rho\int d\mathbf{r}c + a\rho\int d\mathbf{r}h\\ - a\rho^2\left(\int d\mathbf{r}h\right)\left(\int d\mathbf{r}c\right) + a + b\Big\}\end{aligned} \tag{D5}$$

While Eqs. (D1) and (D5) are not in perfect agreement, they are quite similar.

[1] L. S. Ornstein and F. Zernike, Proc. Natl. Acad. Sci. USA **7**, 793 (1914)
[2] R. Evans, Adv. in Phys. **28**, 143 (1979)
[3] D. Chandler and H. C. Andersen, J. Chem. Phys. **57**, 1930 (1972)
[4] F. Hirata and P. J. Rossky, Chem. Phys. Lett. **83**, 329 (1981)
[5] J. Perkyns and B. M. Pettitt, J. Chem. Phys. **97**, 7656 (1992)
[6] D. Beglov and B. Roux, J. Phys. Chem. B **101**, 7821 (1997)
[7] A. Kovalenko and F. Hirata, J. Chem. Phys. **110**, 10095 (1999)
[8] L. Blum and A. J. Torruella, J. Chem. Phys. **56**, 303 (1972)

[9] L. Blum, J. Chem. Phys. **57**, 1862 (1972)
[10] S. Zhao, R. Ramirez, R. Vuilleumier, and D. Borgis, J. Chem. Phys. **134**, 194102 (2011)
[11] L. Verlet, Mol. Phys. **41**, 183 (1980)
[12] L. Verlet and D. Levesque, Mol. Phys. **46**, 969 (1982)
[13] G. A. Martynov and G. N. Sarkisov, Mol. Phys. **49**, 1495 (1983)
[14] F. J. Rogers and D. A. Young, Phys. Rev. A **30**, 999 (1984)
[15] G. Zerah and J. Hansen, J. Chem. Phys. **84**, 2336 (1986)
[16] P. Ballone, G. Pastore, G. Galli, and D. Gazzillo, Mol. Phys. **59**, 275 (1986)
[17] G. A. Martynov and A. G. Vompe, Phys. Rev. E **47**, 1012 (1993)
[18] D. Duh and A. D. J. Haymet, J. Chem. Phys. **103**, 2625 (1995)
[19] L. L. Lee, J. Chem. Phys. **103**, 9388 (1995)
[20] R. Kjellander and S. Sarman, J. Chem. Phys. **90**, 2768 (1989)
[21] O. E. Kiselyov and G. A. Martynov, J. Chem. Phys. **93**, 1942 (1990)
[22] X. S. Chen, F. Forstman, and M. Kasch, J. Chem. Phys. **95**, 2832 (1991)
[23] L. L. Lee, J. Chem. Phys. **97**, 8606 (1992)
[24] S. M. Kast, Phys. Rev. E **67**, 041203 (2003)
[25] S. M. Kast and T. Kloss, J. Chem. Phys. **129**, 236101 (2008)
[26] T. Morita, Prog. Theor. Phys. **20**, 920 (1958)
[27] I. S. Joung, T. Luchko, and D. A. Case, J. Chem. Phys. **138**, 044103 (2013)
[28] D. S. Palmer, A. I. Frolov, E. L. Ratkova, and M. V. Fedorov, J. Phys.: Cond. Matt. **22**, 492101 (2010)
[29] V. Sergiievskyi, G. Jeanmairet, M. Levesque, and D. Borgis, J. Chem. Phys. **143**, 184116 (2015)
[30] V. Sergiievskyi, G. Jeanmairet, M. Levesque, and D. Borgis, J. Chem. Phys. Lett. **5**, 1935 (2014)
[31] J. Johnson, D. A. Case, Y. Yamazaki, S. Gusarov, A. Kovalenko, and T. Luchko, J. Phys.: Cond. Matt. **28**, 344002 (2016)
[32] N. Choudhury and S. K. Ghosh, J. Chem. Phys. **116**, 8517 (2002)
[33] H. C. Andersen, D. Chandler, and J. D. Weeks, J. Chem. Phys. **56**, 3812 (1972)
[34] J. P. Hansen, Phys. Rev. A **2**, 221 (1970)
[35] M. Thol, G. Rutkai, A. Köster, R.Lustig, R. Span, and J. Vrabec, J. Phys. Chem. Ref. Data **45**, 023101 (1916)
[36] D. A. McQuarrie, *Statistical Mechanics*, University Press Books, (2010)
[37] J.-P. Hansen and I. R. McDonald, *Theory of Simple Liquids*, Academic Press, (2006)
[38] T. Morita and K. Hiroike, Prog. Theor. Phys. **23**, 1003 (1960)
[39] J. D. Weeks, D. Chandler, and H. C. Andersen, J. Chem. Phys. **54**, 5237 (1971)
[40] J. G. Kirkwood, J. Chem. Phys. **3**, 300 (1935)
[41] J. G. Kirkwood, J. Chem. Phys. **19**, 275 (1936)
[42] D. Levesque and L. Verlet, Phys. Rev. **182**, 307 (1969)
[43] R. O. Watts, J. Chem. Phys. **50**, 984 (1969)
[44] P. Attard and G. N. Patey, J. Chem. Phys. **92**, 4970 (1990)
[45] J. Perkyns and B. M. Pettitt, Theor. Chem. Acc. **96**, 61 (1997)
[46] E. Lomba and L. L. Lee, Int. J. Thermo. **17**, 663 (1996)
[47] L. L. Lee, D. Ghonasgi, and E. Lomba, J. Chem. Phys. **104**, 8058 (1996)
[48] A. G. Vompe and G. A. Martynov, J. Chem. Phys. **100**, 5249 (1994)
[49] S. J. Singer and D. Chandler, Mol. Phys. **55**, 621 (1985)
[50] A. B. Schmidt, J. Chem. Phys. **99**, 4225 (1993)
[51] G. Sarkisov, J. Chem. Phys. **114**, 9496 (2001)
[52] N. Jakse and I. Charpentier, Phys. Rev. E **67**, 061203 (2003)
[53] J. M. Bomont, J. Chem. Phys. **119**, 11484 (2003)
[54] M. Zacharias, T. P. Straatsma, and J. A. McCammon, J. Chem. Phys. **100**, 9025 (1994)
[55] MATLAB, *version 8.50. (R2015a)*, The MathWorks Inc., Natick, Massachusetts, (2015)
[56] T. Fujita and T. Yamamoto, J. Chem. Phys. **147**, 014110 (2017)
[57] M. Misin, M. V. Fedorov, and D. S. Palmer, J. Chem. Phys. **142**, 091105 (2015)
[58] J.-F. Truchon, B. M. Pettitt, and P. Labute, J. Chem. Theor. Comp. **10**, 934 (2014)
[59] D. Roy, N. Blinov, and A. Kovalenko, J. Phys. Chem. B **121**, 9268 (2017)
[60] T. Luchko, N. Blinov, G. C. Limon, K. P. Joyce, and A. Kovalenko, J. Comp. Aid. Mol. Des. **30**, 1115 (2016)
[61] W. Huang, N. Blinov, and A. Kovalenko, J. Phys. Chem. B **119**, 5588 (2015)
[62] M. Misin, D. S. Palmer, and M. V. Fedorov, J. Phys. Chem. B **120**, 5724 (2016)
[63] H. J. C. Berendsen, J. R. Grigera, and T. P. Straatsma, J. Phys. Chem. **91**, 6269 (2087)
[64] F. Hirata, *Molecular Theory of Solvation*, Kluwer Academic Publishers, Dordrecht, (2003)
[65] B. C. Eu and K. Rah, J. Chem. Phys. **111**, 3327 (1999)